Sociedade Brasileira de Automática (SBA)
XV Simpósio Brasileiro de Automação Inteligente - SBAI 2021, 17 a 20 de outubro de 2021

Modeling, parameter estimation, and control of an aero-pendulum

Ellen R. Lucena * **Saulo O. D. Luiz** * **Antonio M. N. Lima** *

* *Departamento de Engenharia Elétrica,*
Universidade Federal de Campina Grande, PB,
(e-mail: ellen.lucena@ee.ufcg.edu.br,{saulo,amnlima}@dee.ufcg.edu.br).

Abstract: In this work, we propose an aero-pendulum control system design method. We have proposed the aero-pendulum dynamic model employing Newton's second law of motion, the dynamic model of the DC motor, and the thrust model. We have estimated the model parameters by designing the experiments, acquiring the data, applying a nonlinear optimization algorithm for the parameter estimation, and performing the model validation. We have designed the aero-pendulum control system by first linearizing the nonlinear aero-pendulum model by small-signal analysis and designing a linear controller. We have verified the designed aero-pendulum control system by both simulations and experiments. We have concluded that the control system of a didactic aero-pendulum can be developed by means of our proposed design method.

Keywords: aero-pendulum; control; didactics; identification; linearization.

1. INTRODUCTION

Engineering students must develop technical skills such as designing and conducting experiments, identifying, formulating and solving engineering problems while seeking permanent learning. Specifically, undergraduate students of introductory control systems courses need experimental platforms to understand dynamic systems, apply system identification techniques, and design controllers. For example, some concepts in this area can only be completely understood when used in practice, like the relationship between the dynamics of the controlled process and the closed-loop dynamics.

In 2012, at the University of Arizona, Enikov (2012) developed and commercialized a portable structure of an aero-pendulum to facilitate the teaching of automatic control methods for students outside of electrical engineering and mechatronics courses. In this structure, the aero-pendulum position is measured by a potentiometer and is controlled by the association of a controller and a compensator. Other authors have also studied the aero-pendulum position control problem. Kizmaz et al. (2010) applied the technique of sliding mode control to the case of the aero-pendulum, approximating the nonlinear system by a linear system for angles in $[0°, 60°]$ range. Mohammadbagheri and Yaghoobi (2011) designed a PID controller employing the Ziegler-Nichols method, linearizing the nonlinear model using the $\sin\theta \approx \theta$ approximation, which is limited to a small range of values of θ and cannot contemplate the range of angles that will be applied to the aero-pendulum in our work.

The main contribution in our work is the aero-pendulum control system design method. We investigate deeply how a standard control system design process may be applied to a didactic aero-pendulum platform. This investigation gave rise to a specific model, parameter estimation method, specification definition, and controller design for the aero-pendulum.

This paper is organized as follows: in Section 2, the aero-pendulum nonlinear dynamic model and the experimental platform are presented; the model parameter estimation by means of the experiment design, data acquisition, a nonlinear optimization algorithm for the parameter estimation, and the model validation were described in Section 4; the control system specifications, and the aero-pendulum control system design are presented in Section 5; finally, the simulation and experimental results of the proposed control system were evaluated in Section 6.

2. THE DYNAMIC MODEL OF THE AERO-PENDULUM

In this section, the aero-pendulum nonlinear dynamic model is first presented and then such model is analyzed in steady-state. An aero-pendulum is depicted in Figure 1. It is composed of a rotating rod of length L, connected to a bearing at one end, and a DC motor at the other end; the rotor of the DC motor is attached to a gearbox: the driver gear is connected to the rotor and the driven gear is connected to a propeller. The angular displacement of the aero-pendulum is due to the thrust T to which the propellers are subjected. The thrust causes a torque TL in the pendulum, causing a change in its angular position, represented as the angle y between the rod and the vertical axis. This displacement causes the force weight mg to have a component $mg\sin(y)$ perpendicular to the rod. The component $mg\sin(y)$ of the weight force is considered to be applied to the center of mass of the set {rod, motor, gears, propeller}, whose distance to the bearing is d.

The thrust, on the other hand, is provided by the angular speed of the driven gear, coupled to the propeller axis.

⋆ The authors are grateful for the financial support provided by PPgEE/UFCG, CAPES and CNPq.

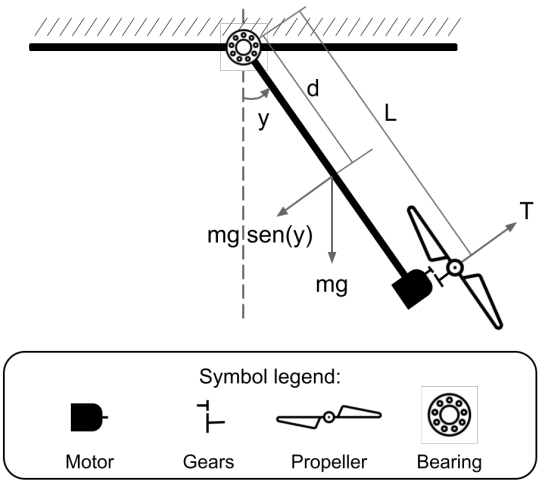

Figure 1. Illustration of the aero-pendulum platform and its basic set of components: {bearing, rod, motor, gears, propeller}.

Such an angular speed depends directly on the rotor speed. The motor is powered by a voltage source controlled by a PWM signal with duty cycle u.

The motor armature equivalent circuit is represented by a series association of the voltage source v_a, the armature resistance R_a, the armature inductance L_a, and the back electromotive force $K_\omega \omega_1$, where K_ω is the electromotive constant, and ω_1 is the rotor angular speed. The voltage source is $v_a = K_f u$, where u is the PWM duty cycle, and K_f is constant. The differential equation for the armature current i_a is presented in (1), according to Franklin et al. (2001). The differential equation for the rotor speed is shown in (2), Franklin et al. (2001), where the electromagnetic torque is given by $K_i i_a$, the torque due to the viscous friction by $F\omega_1$, and the mechanical torque imposed by the gears and the propeller by T_1.

$$\frac{di_a}{dt} = -\frac{R_a}{L_a} i_a - \frac{K_w}{L_a}\omega_1 + \frac{1}{L_a} v_a \tag{1}$$

$$\frac{d\omega_1}{dt} = \frac{K_i}{J_m} i_a - \frac{F}{J_m}\omega_1 - \frac{1}{J_m} T_1 \tag{2}$$

The rotor applies a torque T_1 to the driver gear, which produces the torque T_2 to the propeller. Considering the number of teeth N_1 and N_2 respectively of the driver and the driven gears, the angular speed of the propeller $\omega_2 = (N_1/N_2)\,\omega_1$ and the torque applied to the propeller is $T_2 = (N_2/N_1)\,T_1$.

Employing Newton's second law of motion, the differential equation for the pendulum rotational motion is presented in (3), Franklin et al. (2001), where J is the moment of inertia of the set {rod, motor, gears, propeller}, y is the angular position of the rod in relation to the vertical axis, C is the viscous friction coefficient, m is the mass of the set {rod, motor, gears, propeller}, d is the distance from the bearing to the center of mass of the set, L the distance between the bearing and the propeller axis, illustrated in Figure 1, and $T = K_T w_2^2$ is the thrust.

$$J\ddot{y} + C\dot{y} + mgd\sin(y) = LT \tag{3}$$

The state-space representation of the aero-pendulum model is presented in (4) and (5), where Ω is the aero-pendulum angular speed.

$$\frac{dy}{dt} = \Omega \tag{4}$$

$$\frac{d\Omega}{dt} = -\frac{mgd}{J}\sin(y) - \frac{C}{J}\Omega + \frac{L}{J}T \tag{5}$$

In this work, the following *assumptions* are considered:

(1) the motor dynamics represented by (1) and (2) is fast enough to be neglected with regard to the pendulum dynamics represented by (3);
(2) the moment of inertia of the propellers J_h is neglected and the transient response of the propellers is considered to be much faster than that of the pendulum rod. The propellers are then considered to be in equilibrium, with constant speed $\omega_2 = \omega_{2_{ss}}$;
(3) the motor shaft angular velocity assumes only non-negative values $\omega_1 \geq 0$.

By considering these assumptions, the dynamics between the duty cycle u and the thrust T may be neglected. In the next section, we present how the constant thrust T_{ss} is related to a constant duty cycle u_{ss}. Then we show that, in steady-state, a constant thrust T_{ss} may be directly evaluated from the constant angular position y_{ss}.

2.1 The steady-state

When a PWM signal with constant duty cycle $u = u_{ss}$ is applied, the motor axis rotates with constant angular speed $\omega_{1_{ss}}$, and therefore the propeller axis also rotates with constant angular speed $\omega_{2_{ss}}$, producing constant thrust $T = T_{ss}$. By considering that (1) and (2) are in steady-state, the thrust T_{ss} as a function f_T of the PWM duty cycle u_{ss} is given by:

$$T_{ss} = f_T(u_{ss}) = K_0\left(-K_1 + \sqrt{K_1^2 + K_2 u_{ss}}\right)^2. \tag{6}$$

where, $K_0 = \frac{K_T}{4K_Q^2}\left(\frac{N_1}{N_2}\right)^{-4}$, $K_1 = \left(\frac{K_i K_w}{R_a} + F\right)$, and $K_2 = \frac{4K_Q K_i K_f}{R_a}\left(\frac{N_1}{N_2}\right)^3$, where K_Q is the aerodynamic drag constant and K_T is the lift constant (Corke, 2017, p. 115). The function $f_T : [0, 100] \to \mathbb{R}^+$, $T_{ss} = f_T(u_{ss})$, in (6) is in this work denoted as *thrust function*. Its inverse $f_T^{-1} : \mathbb{R}^+ \to [0, 100]$, $u_{ss} = f_T^{-1}(T_{ss})$, is presented in (7) and will be applied for *control allocation*.

$$u_{ss} = f_T^{-1}(T_{ss}) = \frac{\left(\sqrt{\frac{T_{ss}}{K_0}} + K_1\right)^2 - K_1^2}{K_2} \tag{7}$$

Considering the pendulum in steady state for a constant thrust $T = T_{ss}$, and replacing $\Omega = 0$, $\frac{d\Omega}{dt} = 0$, and $y = y_{ss}$ in (5), we have:

$$mgd\sin(y_{ss}) = LT_{ss} \Rightarrow T_{ss} = \frac{mgd\sin(y_{ss})}{L}. \tag{8}$$

From (8), is shown that a constant thrust T_{ss} can be estimated from a constant angular position y_{ss}, which can be measured by a sensor of angular position.

3. EXPERIMENTAL PLATFORM

Photographs of the experimental platform are shown in Figure 2. The mechanical parts are a mast, a support and a base made of polystyrene, a bearing, a solid cylinder, and a metal rod. We have used a rigid rod, made of iron coated with ceramic material, to avoid vibration. The propulsion system is composed of a power source, a motor Shield (a dual full-bridge driver), a DC motor, a gearbox, and a propeller. The pendulum angular position is measured by means of a magnetic position sensor, the AS5040. The target platform is an Arduino Mega. During operation, a development computer (not presented in Figure 2) commands input signals the Arduino acquires the angular position by a USB cable.

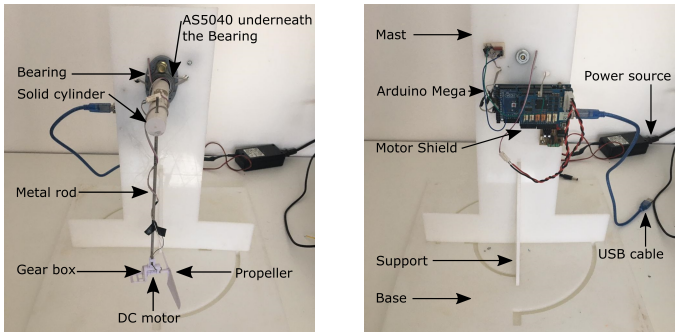

(a) Photograph of the aero-pendulum front.

(b) Photograph of the aero-pendulum rear.

Figure 2. Photographs of the experimental platform.

The experimental platform software was developed in Simulink as the block diagram shown in Figure 3, where the duty cycle u is the input of a block that commands a PWM port in the Arduino board. A digital output is set to 1 for selecting the anticlockwise direction for the propeller. The angular position y is acquired by means of the block `sfun_as5040_aeropendulo` developed by de Araújo (2021). The target code can be automatically generated from the Simulink model, cross-compiled, and downloaded into the Arduino Mega by means of a USB cable.

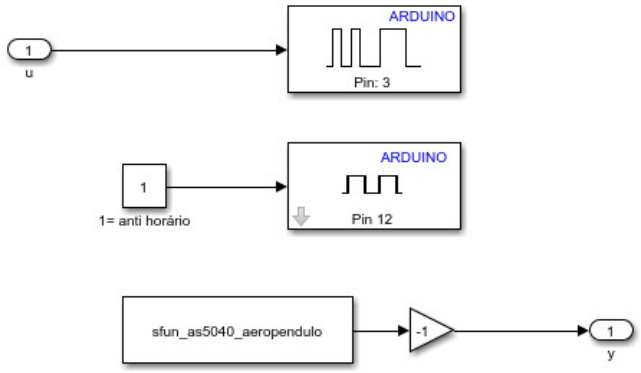

Figure 3. Simulink model of the process.

4. PARAMETER ESTIMATION

To analyze the open-loop dynamics of a process and design a closed-loop control system, it is required to identify the model of the process and estimate the model parameters. For the case of the aero-pendulum, the parameters of the differential equation in (3) and the function in (6) were estimated.

4.1 Thrust function estimation

To estimate the thrust function f_T parameters in (6), 15 experiments were carried out. In each experiment, a PWM duty cycle u was applied to the aero-pendulum for 50 seconds, so that the steady-state could be achieved. We have used the following duty cycle values {0%, 4%, 8%, 12%, ... , 60%}. The angular position values at steady-state were measured and saved. The steady state angular position y_{ss} was evaluated as the average of the acquired angular position values is steady-state. The estimated parameters were $K_0 = 0.0072653$, $K_1 = 0.5798$, $K_2 = 0.3745$.

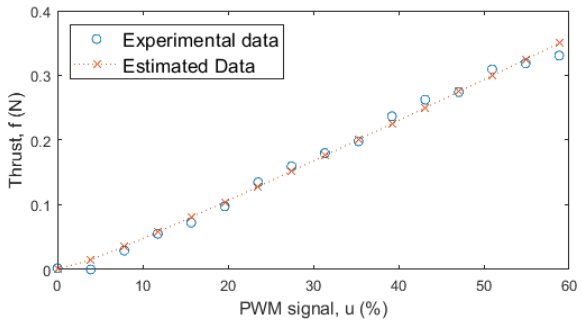

Figure 4. The thrust T_{ss} as a function of the PWM duty cycle u_{ss}: experimental data, and data estimated by means of (6).

The estimated and experimental values of the thrust are shown in Figure 4. For this estimate, a mean squared error of $MSE = 8.1630 \cdot 10^{-5} N^2$ was obtained. The estimated model was then considered satisfactory.

4.2 Parameter estimation of the pendulum model

To estimate the parameters of the differential equation presented in (3), experiments were performed by applying the input represented in (9), where N corresponds to the number of frequency components of the input spectrum, which was chosen as 64. In each experiment, the input was applied for 120 seconds. A gain of 5 and an *offset* of 55 were chosen.

$$u(t) = \frac{100}{255}\left\{55 + 5\sum_{j=0}^{N-1} c\left[\left(\omega_m + j\frac{\Delta\omega}{N}\right)t - j(j+1)\frac{\pi}{N}\right]\right\}$$

where, c is cosine, and $\Delta\omega = \omega_M - \omega_m$, with $\omega_M = 50Hz$ e $\omega_m = 0.5Hz$.

Before estimating the parameters, the model was first represented in discrete time. We used the finite difference

forward Euler method, for approximating the first and second order derivatives of the pendulum angular position:

$$\dot{y}(t) \approx \frac{y(t+h) - y(t)}{h}, \tag{9}$$

$$\ddot{y}(t) \approx \frac{y(t+2h) - 2y(t+h) + y(t)}{h^2}, \tag{10}$$

where h is the sampling interval. Replacing $\dot{y}$ and $\ddot{y}$ respectively by the expressions (9) and (10) in (3), we have:

$$\begin{aligned} y(t) = \frac{C}{J}\left[-hy(t-h) + hy(t-2h)\right] + \\ +2y(t-h) - y(t-2h) + \\ +\frac{1}{J}\left[-h^2 mgd\sin(t-2h) + \frac{h^2 L}{J}T(t-2h)\right] \end{aligned} \tag{11}$$

Some of the parameters in (11) were measured, such as m, d and L. The sampling period $h = 0.05$s, due to the interrupt service routine in the Arduino board for acquiring the angular position from the AS5040 magnetic position sensor, and the communication between the Arduino and the development computer. Thus, we have estimated the missing parameters, namely C and J. The parameter vector to be estimated is $\theta = [\, C/J \;\; 1/J \,]^T$. By writing the model output in (11) as $\hat{y}(t|\theta)$, we emphasize that it is estimated from experimental data and it depends on the parameters.

The estimation problem was defined in (12), where one seeks to find the set of parameters θ that minimizes the quadratic estimation error between the experimental data $y(t_k)$ and the model output $\hat{y}(t_k|\theta)$, where the sampling instants are $t_k = kh$, $k = 1, 2, \ldots, K$, θ_{lb} and θ_{ub} are respectively lower and upper bounds for θ, and $[\, \theta_{lb} \;\; \theta_{ub} \,]$ is a 2-dimensional interval.

$$\hat{\theta} = \underset{\theta \in \mathbb{D}}{\operatorname{argmin}} \frac{1}{2} \sum_{k=1}^{K} \left[y(t_k) - \hat{y}(t_k|\theta) \right]^2, \tag{12}$$

$$\mathbb{D} \subseteq \mathbb{R}^2_{>0} \cap [\, \theta_{lb} \;\; \theta_{ub} \,]$$

To solve this estimation problem, a non-linear convex optimization method was used because (11) is not written as the product of a regression vector and a parameter vector; C and J are positive; and the initial value J_0 of the moment of inertia may be calculated before the estimation process. The moments of inertia of the solid cylinder, the rod, and the set {motor, gears, propeller} are respectively $\frac{m_c r_c^2}{2}$, $\frac{m_r L^2}{3}$, and $m_p L^2$, where the solid cylinder mass $m_c = 0.030$kg, its radius is $r_c = 0.01$m, the rod mass $m_r = 0.016$kg, the rod length $L = 0.23$m, the {motor, gears, propeller} total mass $m_p = 0.005$kg. Thus the initial value of the moment of inertia is $J_0 = \frac{m_c r_c^2}{2} + \frac{m_r L^2}{3} + m_p L^2$. The vector of initial values is $\theta_0 = [\, 0 \;\; 1/J_0 \,]$.

We have also defined upper and lower bound values for J, respectively as 90% and 110% of the initial value. The vectors of lower and upper bounds are respectively $\theta_{lb} = [\, 0 \;\; 0.9/J_0 \,]$ and $\theta_{ub} = [\, \infty \;\; 1.1/J_0 \,]$.

The weight of the solid cylinder is balanced by a normal force from the bearing. Thus the solid cylinder does not contribute to m, which is $m = m_r + m_p = 0.021kg$. The local gravitational acceleration is $g = 9.806\text{m/s}^2$, and $d = 0.160$m. The solution of the proposed estimation problem was the parameter vector $\theta = [\, 0.689 \;\; 1824.372 \,]$. Thus, $C = 3.719 \cdot 10^{-4}\text{N} \cdot \text{m} \cdot \text{s/rad}$, and $J = 5.481 \cdot 10^{-4}\text{kg} \cdot \text{m}^2$. The estimation data and the validation data are shown in Figure 5. The mean squared error between the validation output and the estimated output is approximately 4.678°^2}.

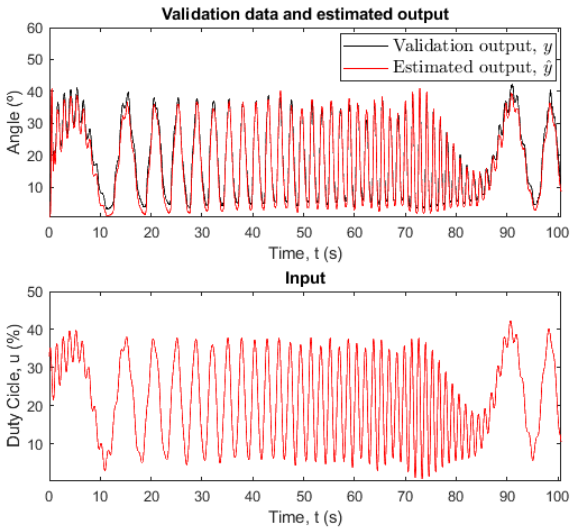

Figure 5. Result of the estimation problem: (a) the estimated output and the validation output signal; (b) validation input signal.

After estimating the aero-pendulum model parameters and validating the model, we have designed a control system for evaluating the closed-loop performance of the aero-pendulum. The control system design process is presented in the next section.

5. CONTROL SYSTEM DESIGN

The aero-pendulum control system shown in Figure 6 is composed of a linear controller and the control allocation. The inputs of the linear controller are the reference angular position r and the measured angular position y_S. The output of the linear controller is the commanded thrust T_c. The duty cycle u to be applied to the propulsion system is evaluated by means of the inverse function in (7), implemented in the control allocation. We have designed the control system by: first, defining the closed-loop specification; second, linearizing the model in (4) and (5); and then designing a linear controller.

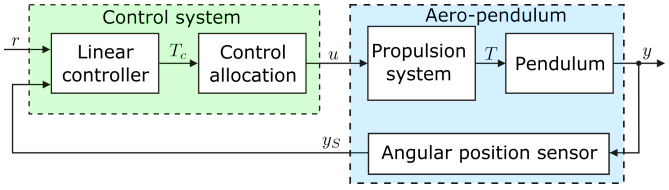

Figure 6. Control system block diagram.

5.1 Specifications

To define the closed-loop specifications, we have initially investigated the physical limits and constraints of the aero-pendulum.

From experimental data, the fastest open-loop response was achieved to a 58.8% step input at the duty cycle, shown in Figure 7. We have used this transient response to determine the fastest rise, accommodation, and peak times that the aero-pendulum is able to achieve.

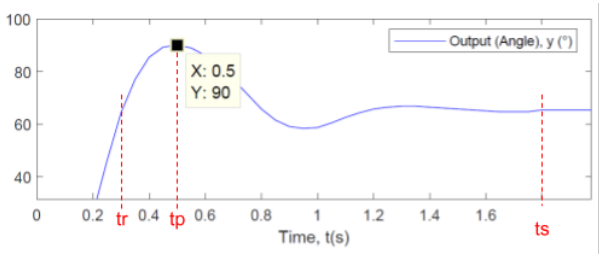

Figure 7. Open-loop transient response to a 58.8% step input at the duty cycle u.

In Figure 7, the rise, peak and settling [1] times are respectively $t_r \approx 0.3$s, $t_p \approx 0.5$s and $t_s \approx 1.6$s. The maximum angular position achieved is 90°, which is considered a safe maximum angle for avoiding a 360° turn. The steady-state angular position is approximately 65°. Thus, the overshoot $M = 38.46\%$. Therefore, the closed-loop specifications presented in Table 1 must satisfy those aero-pendulum physical limits and constraints.

Table 1.

ID	Description
P1.1	When the reference is a step, the percent overshoot shall be less than or equal to 38.46%.
P1.2	When the reference is a step, the rise time shall be greater than or equal to 0.3s.
P2.1	When the reference is a step, the peak time shall be greater than or equal to 0.5s.
P2.2	When the reference is a step, the settling time shall be greater than or equal to 1.6s. and less than or equal to 10s.

5.2 Controller Design

Linearizing the model presented in (4) and (5) for a given angular position y_0 by small-signal analysis, as presented by Franklin et al. (2001), the linearized model in space state is

$$\frac{d\Delta y}{dt} = \Delta\Omega \tag{13}$$

$$\frac{d\Delta\Omega}{dt} = -\frac{mgd}{J}\cos(y_0)\Delta y - \frac{C}{J}\Delta\Omega + \frac{L}{J}\Delta T, \tag{14}$$

whose equivalent transfer function is

$$H(s) = \frac{\Delta Y(s)}{\Delta T(s)} = \frac{\frac{L}{J}}{s^2 + \frac{C}{J}s + \frac{mgd}{J}\cos y_0}, \tag{15}$$

[1] The time, in seconds, taken for the output to be greater than or equal to 99% of the final value and less than or equal to 101% of the final value.

and the equivalent differential equation is

$$\Delta\ddot{y} + \frac{C}{J}\Delta\dot{y} + \frac{mgd}{J}\cos y_0 \cdot \Delta y = \frac{L}{J}\Delta T. \tag{16}$$

Considering the linearized model in (15), a PID controller was designed by means of the pole-zero cancellation technique. The PID transfer function is:

$$G(s) = k_p + \frac{k_i}{s} + k_d s = \frac{k_d\left(s^2 + \frac{k_p}{k_d}s + \frac{k_i}{k_d}\right)}{s}. \tag{17}$$

Comparing (17) and (15), the process poles may be canceled by the controller zeros by setting

$$\frac{k_p}{k_d} = \frac{C}{J} \tag{18}$$

$$\frac{k_i}{k_d} = \frac{mgd}{J}\cos y_0 \tag{19}$$

After the pole-zero cancellation, the resulting closed-loop transfer function is

$$\frac{\Delta Y(s)}{\Delta R(s)} = \frac{k_d L/J}{s + k_d L/J} \tag{20}$$

The resulting closed-loop system is a first-order system. Then the specifications P1.1, P1.2, and P1.3 in Table 1 should be satisfied. The derivative gain k_d may be used to allocate the closed-loop pole. By choosing the closed-loop settling time as 5.5s, the specification P2.2 should also be satisfied. The derivative gain must satisfy

$$1 - e^{\frac{k_d L}{J}5.5} = 0.99. \tag{21}$$

Thus $k_d = 0.002$, $k_i = 0.1202$ and $k_p = 0.0014$. The PID was implemented with the filtered derivative action in (22). The continuous-time transfer function was discretized $G(s)$ by means of the Zero-order hold method. The discrete time controller transfer function $G(z)$ is shown in (23).

$$G(s) = 0.0014 + \frac{0.1202}{s} + \frac{0.2s}{s + 100} \tag{22}$$

$$G(z) = \frac{0.20138z^2 - 0.39538z + 0.19997}{z^2 - 1.0067z + 0.0067379} \tag{23}$$

The designed control system was verified by both simulations and experiments. The verification results are presented in the next section.

6. VERIFICATION

First, we have verified the designed control system by means of simulations. We have implemented the block diagram shown in Figure 8 as the Simulink model shown in Figure 9. Considering the simulation results presented in Figure 11, the closed-loop specifications presented in Table 1 were satisfied.

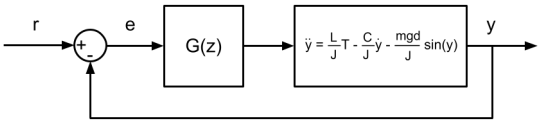

Figure 8. Block diagram representing the aero-pendulum control system.

Secondly, we have verified the designed control system experimentally by means of the aero-pendulum platform.

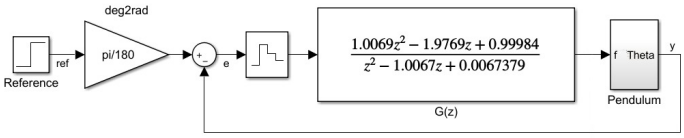

Figure 9. Simulink model for simulating the aero-pendulum control system.

We have implemented the block diagram shown in Figure 6 as the Simulink model shown in Figure 10. Both simulation and experimental results are presented in Figure 11. The transient response and the steady-state in simulation and experimental results are similar for the error $e(t)$ and the angle $y(t)$. But the steady-state in simulation and experimental results are different for the thrust $T(t)$ and the duty cycle $u(t)$, possibly because of prediction errors of the thrust T_{ss} as a function f_T of the PWM duty cycle u_{ss} in (6). However, the closed-loop specifications presented in Table 1 were satisfied.

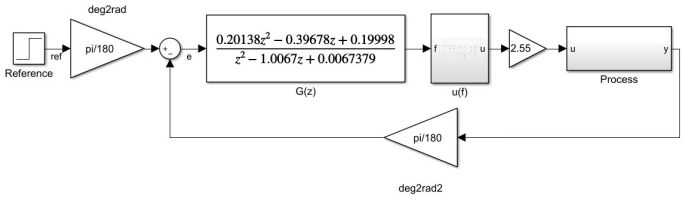

Figure 10. Simulink model of the aero-pendulum control system for experimental verification.

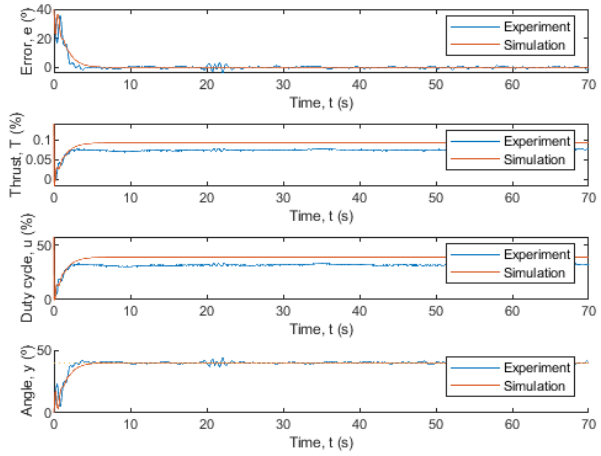

Figure 11. Simulation and experimental results of the verification process.

7. CONCLUSION

In this work, we have concluded that the control system of a didactic aero-pendulum can be developed by means of our proposed design method. The process model may be represented as a series composition of a thrust function representing the propulsion system and a nonlinear model representing the pendulum. The process model parameters can be estimated by a non-linear convex optimization method with constraints on the parameters. The control system can be composed of a linear controller and control allocation. The controller can be designed by: (i) linearizing the non-linear pendulum model; (ii) applying the pole-zero cancellation technique; and (iii) discretizing the controller transfer function by means of the zero-order hold method. The controller software may be developed and verified by means of Simulink models: (i) a Simulink model of the controller may be developed and then verified by simulations; (ii) from the controller Simulink model, code can be automatically generated, cross-compiled and downloaded into the target platform; (iii) the controller software running in the target platform can be verified by experiments. We expect to use the didactic aero-pendulum as an experimental platform in Control System courses both at undergraduate and graduate levels. We have already successfully used this didactic aero-pendulum in a graduate course of the PPgEE/UFCG. Several topics may be studied by means of the proposed platform, such as Modeling, System identification, Controller Design, Model-based design, automatic code generation, the V-model, and Verification&Validation. For future works, we plan to improve the estimation of the thrust function to attenuate the errors between the simulation and experimental results in steady-state; and to linearize the process model by means of the Feedback Linearization.

ACKNOWLEDGMENT

The authors are grateful for the financial support provided by PPgEE/UFCG, CAPES and CNPq.

REFERENCES

Corke, P. (2017). *Robotics, Vision and Control: Fundamental Algorithms In MATLAB, Second Edition*. Springer Publishing Company, Incorporated, India, 2nd edition.

de Araújo, J.R.C. (2021). *Fabricação, modelagem e controle de uma junta antagônica acionada por atuador de náilon retorcido*. Master's thesis, UFCG, Campina Grande, Brasil.

Enikov, E.T. (2012). Mechatronic aeropendulum: Demonstration of linear and nonlinear feedback control principles with matlab/simulink real-time windows target. *IEEE Transactions on Education*, 55(4).

Franklin, G.F., Powell, D.J., and Emami-Naeini, A. (2001). *Feedback Control of Dynamic Systems*. Prentice Hall PTR, USA, 4th edition.

Kizmaz, H., Aksoy, S., and Muhurcu, A. (2010). Sliding mode control of suspended pendulum. 1 – 6.

Mohammadbagheri, A. and Yaghoobi, M. (2011). A new approach to control a driven pendulum with pid method. 207–211.